Bull. Chem. Soc. Ethiop. **2018**, 32(3), 437-450.
ISSN 1011-3924
Printed in Ethiopia

DOI: https://dx.doi.org/10.4314/bcse.v32i3.3

SYNTHESIS, SPECTRAL, THERMAL, KINETIC AND ANTIBACTERIAL STUDIES OF TRANSITION METAL COMPLEXES WITH BENZIMIDAZOLYL-2-HYDRAZONES OF *o*-HYDROXYACETOPHENONE, *o*-HYDROXYBENZOPHENONE AND *o*-VANILLIN

Ranjan K. Mohapatra[1*], Pradeep K. Das[2], Marei M. El-ajaily[3], Umakanta Mishra[4] and Dhruba C. Dash[4]

[1]Department of Chemistry, Government College of Engineering, Keonjhar-758002, Odisha, India
[2]Department of Chemistry, N.C. Autonomous College, Jajpur-755001, India
[3]Chemistry Department, Faculty of Science, Benghazi University, Benghazi, Libya
[4]School of Chemistry, Sambalpur University, Jyoti Vihar, Burla, Sambalpur-768019, Odisha, India

(Received July 27, 2017; Revised November 4, 2018; Accepted November 9, 2018)

ABSTRACT. A novel series of Schiff base metal complexes of the type $[M(L)_2].nH_2O$, where L= 2-(α-methylsalicylidenehydrazino) benzimidazole (L1), 2-(α-phenylsalicylidenehydrazino)benzimidazole (L2), 2-(*o*-vanillinidenehydrazino)benzimidazole (L3), M = Cu(II), Co(II), Ni(II) and Zn(II), have been synthesized and characterized. The results are in consistent with tridentate chelation of ligand with azomethine nitrogen, ring nitrogen and a deprotonated phenolic oxygen atom. All these compounds have been screened for their antibacterial activities against *B. subtilis*, *B. stearothermophilus*, *E. coli* and *S. typhi*.

KEY WORDS: Schiff base, Metal complexes, Spectral studies, Thermal studies, Kinetic studies, Antibacterial studies

INTRODUCTION

Benzimidazole is a bicyclic compound having imidazole ring containing two nitrogen atoms at alternate positions fused to the benzene ring. It is an important biologically active heterocyclic compound. The chemistry of benzimidazole and its derivatives has been of great interest to medicinal chemists owing to their remarkable antimicrobial [1], antibacterial [2], antioxidant [3], anticancer [4], anthelmintic [5], cytotoxic [6], analgesic [7], antiulcer [8], antiviral [9] and anticonvulsant [10] activities. The antifungal [11], antimicrobial [12], antioxidant [13] and catalytic [14] activities of transition metal complexes with benzimidazole have also been extensively studied. The benzimidazole metal complexes have been found to display greater effectiveness than free ligands [15-17] from above counts. In recent years considerable attention has also been paid to these metal complexes because of their contribution to cancer therapy [18-19].

Following all these observations and as a part of our ongoing research on coordination chemistry of multidentate ligands [20-23], we have made an effort to synthesize and perform the structural studies on the first-row transition metal complexes with some hydrazone derivatives containing benzimidazole moiety. Moreover, the bio-potency of these compounds has been investigated against *B. subtilis, B. stearothermophilus, E. coli* and *S. typhi*.

*Corresponding author. E-mail: ranjank_mohapatra@yahoo.com

EXPERIMENTAL

Materials and methods

All chemicals and reagents including 2-hydrazinobenzimidazole, *o*-hydroxy acetophenone, *o*-hydroxy benzophenone, *o*-vanillin and the metal salts were obtained from Sigma Aldrich and used without further purification.

Preparation of ligands

Various ligands were prepared by condensing 2-hydrazinobenzimidazole with respective aldehyde and ketone as follows. Ethanolic solution of 2-hydrazinobenzimidazole (0.01 mol in 20 mL) was added to ethanolic solution of *o*-hydroxyacetophenone/*o*-hydroxybenzophenone/*o*-vanillin (0.01 mol in 20 mL), followed by addition of 2 drops of acetic acid to the above mixture. The resulting solution was heated for 2 to 3 hours on a water bath. The clear solution was allowed to evaporate at room temperature and washed with diethyl ether and finally, recrystallized in ethanol. The sample was dried in vacuo over fused calcium chloride and then analyzed.

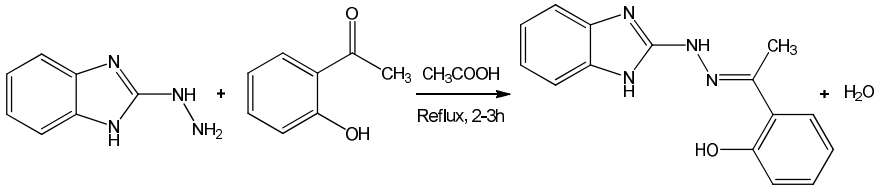

(2-hydrazinobenzimidazole) (*o*-hydroxyacetophenone) (**L1**)

Scheme 1. Procedure for preparation of L1.

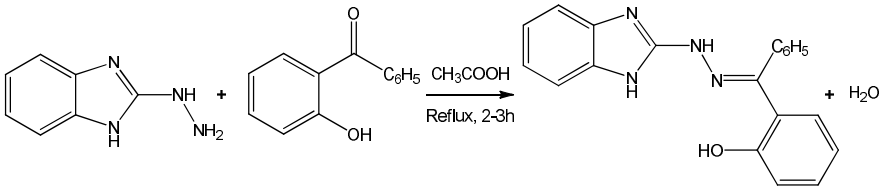

(2-hydrazinobenzimidazole) (*o*-hydroxybenzophenone) (**L2**)

Scheme 2. Procedure for preparation of L2.

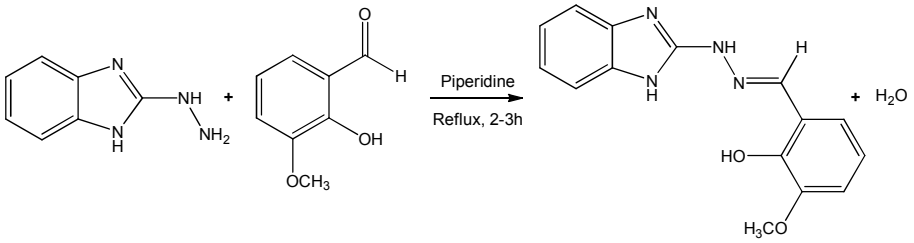

(2-hydrazinobenzimidazole) (*o*-vanillin) (**L3**)

Scheme 3. Procedure for preparation of L3.

Preparation of the complexes

A hot ethanolic solution of the ligand (0.02 mol in 20 mL) was treated with ethanolic solution of respective hydrated metal(II) chloride (0.01 mol in 20 mL) in 2:1 molar ratio. The pH of the resulting mixture was adjusted to 7.5 to 8.0 by adding 0.25 g of solid NaOH. It was refluxed on a water bath for about 2 hours when colored complexes (Figure 1) precipitated out in each case. The precipitates were filtered, washed with ethanol followed by ether and finally dried in vacuo over fused $CaCl_2$.

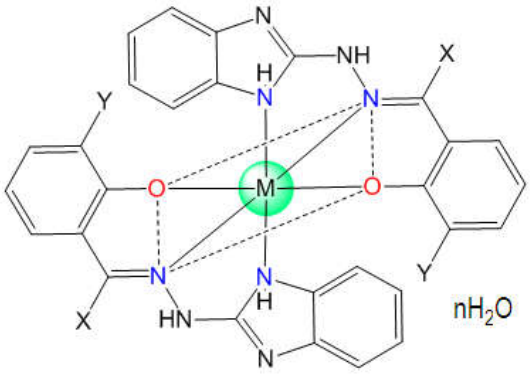

M = Co(II), Ni(II), Cu(II) and Zn(II) X = -H, $-CH_3$, $-C_6H_5$, Y = -H, - OCH_3

Figure 1. Proposed structure of the complexes.

Analysis and physical measurements

The metal contents were determined gravimetrically [24]. The molar conductance measurements were recorded with a Toshniwal Conductivity Bridge (model CL-01-06, cell constant 0.5 cm^{-1}) in DMSO. Microanalyses (C, H, N) were executed by using a MLW-CHN micro analyzer. The room temperature magnetic susceptibility values were determined by Gouy method with mercury tetrathiocyanatocobalt(II), $Hg[Co(SCN)_4]$ as calibrant. The electronic spectra were obtained in DMSO on a Perkin-Elmer spectrophotometer. FTIR spectra as KBr pellets were recorded using Varian FTIR spectrophotometer, Australia. Thermo-gravimetric analysis was done by Netzch-429 thermal analyser in a nitrogen atmosphere with a rate of temperature increase of 10 $^oC\ min^{-1}$. The ^{1}H-NMR and ^{13}C-NMR spectra of the complexes were obtained on JEOL GSX-400 model equipment in DMSO-d_6 medium. The ESR spectra were recorded on an E-112 EPR Spectrophotometer.

In vitro antibacterial activity

The *in vitro* antibacterial activities of the ligands and their metal complexes were studied at 100 µg mL^{-1} concentrations by Agar Well Diffusion Assay Technique [25] against *B. subtilis* (MTCC-121 and NCIM-2250), *B. stearothermophilus* (NCIM-2542 and ATCC-12977) (Gram positive bacteria) and *E. coli* (NCIM-2109 and ATCC-11775), *S. typhi* (MTCC-3224, NCIM-2501 and ATCC-23564) (Gram negative bacteria). Solutions of the compounds in DMSO were plated onto the cultured agar medium and incubated for a period of 24 h at 37 ^oC. After the incubation period, the plates were observed for zones of inhibition (in cm). The standard antibacterial drug ciprofloxacin is also screened as above.

RESULTS AND DISCUSSION

The analytical data and physical properties of the compounds are listed in Table 1, which are in good agreement with the calculated values. These reported metal complexes are coloured, non hygroscopic and soluble in dioxane, DMSO and DMF. They are stable under normal conditions and all of them decompose above 250 ^{o}C.

Table 1. Analytical and physical data of the complexes.

S. No.	Compounds	Color	Yields (%)	Λ_m[a]	C Found (calcd)	H Found (calcd)	N Found (calcd)	M Found (calcd)
1	L1	Grey	80	-	67.64 (67.67)	5.24 (5.26)	21.01 (21.05)	-
2	L2	Light brown	70	-	73.12 (73.17)	4.83 (4.87)	17.04 (17.07)	-
3	L3	Yellow	80	-	63.76 (63.83)	4.92 (4.96)	19.82 (19.86)	-
4	$[Co(L1)_2].H_2O$	Brown	61	11.39	59.28 (59.31)	4.58 (4.61)	18.42 (18.45)	9.65 (9.72)
5	$[Ni(L1)_2].H_2O$	Brick red	62	10.78	59.30 (59.34)	4.59 (4.62)	18.42 (18.46)	9.63 (9.67)
6	$[Cu(L1)_2].2H_2O$	Light green	65	10.49	57.15 (57.18)	4.72 (4.76)	17.74 (17.79)	10.05 (10.10)
7	$[Zn(L1)_2].H_2O$	Light yellow	62	18.21	58.65 (58.69)	4.51 (4.56)	18.22 (18.26)	10.62 (10.70)
8	$[Co(L2)_2].H_2O$	Leaf green	63	11.22	65.44 (65.48)	4.34 (4.37)	15.25 (15.28)	8.01 (8.05)
9	$[Ni(L2)_2].H_2O$	Chocolate	64	12.59	65.48 (65.51)	4.35 (4.38)	15.26 (15.29)	7.96 (8.01)
10	$[Cu(L2)_2].2H_2O$	Olive Green	60	10.31	63.49 (63.53)	4.49 (4.51)	14.79 (14.82)	8.38 (8.41)
11	$[Zn(L2)_2].H_2O$	Light yellow	61	6.51	64.89 (64.92)	4.30 (4.34)	15.11 (15.15)	8.80 (8.84)
12	$[Co(L3)_2].H_2O$	Brown	63	8.20	56.12 (56.16)	4.34 (4.38)	17.44 (17.47)	9.15 (9.20)
13	$[Ni(L3)_2].H_2O$	Grey	60	10.19	56.15 (56.19)	4.35 (4.38)	17.45 (17.48)	9.12 (9.16)
14	$[Cu(L3)_2].2H_2O$	Bluish black	61	8.12	54.23 (54.25)	4.49 (4.53)	16.85 (16.88)	9.52 (9.58)
15	$[Zn(L3)_2].H_2O$	White	63	11.42	55.58 (55.61)	4.29 (4.34)	17.26 (17.30)	10.06 (10.10)

[a]Ohm^{-1} cm^2 $mole^{-1}$.

IR spectra

2-Hydrazinobenzimidazole exhibits a pair of strong bands at ~3310 and ~3275 cm^{-1} which may be assigned to asymmetric and symmetric stretching modes of vibrations of the $-NH_2$ group. Apart from these bands a multiple band system of medium intensity is observed at 3145 and 3100 cm^{-1} which may be attributed to $\nu_{(N-H)}$ of benzimidazolyl group and $\nu_{(N-H)}$ exocyclic, respectively. Further, absorptions of medium intensity are observed at ~1540 cm^{-1} and ~1340 cm^{-1} due to ring stretching vibration modes of cyclic (C=N) and cyclic (C-N) of benzimidazole moiety. The N-H bending vibrations for primary amine occur at 1600-1575 cm^{-1}. The band appearing at 1620 cm^{-1} may be assigned to N-H bending vibrational mode. The bands positioned at ~1230 cm^{-1} and ~1000 cm^{-1} may be due to the C-N (exocyclic) stretching vibrations and N-N stretching vibrations, respectively.

The most significant changes in the IR spectra of the condensation products of 2-hydrazinobenzimidazole with *o*-vanillin, *o*-hydroxyacetophenone or *o*-hydroxy benzophenone are the disappearance of the -NH_2 stretching and bending vibrations. The band at ~3300 cm^{-1} due to phenolic -OH stretching vibration disappears in IR spectra of metal complexes formed by above ligands which clearly demonstrate the deprotonation of phenolic (OH) group and coordination to the metal ion through an oxygen atom. This is further substantiated by the hypsochormic shift of phenolic ν_{C-O} mode around ~1280 cm^{-1} of the free ligand to ~1500 cm^{-1} in the spectra of these complexes. This may be due to partial double bond character assumed by C-O in coordination to the metal ion as a result of drainage of π-electron of benzene ring through resonance. The position of the band due to ν_{N-H} (exocyclic) however, remains practically unaltered in the present complexes indicating non-involvement of imino nitrogen atom in coordination to the metal ion. Further, the non coordination of ring nitrogen atom (-C=N) of benzimidazole moiety in the complexes is also ascertained by finding no change in the positions of the characteristic IR bands at ~ 1540 and ~ 1320 cm^{-1} due to $\nu_{C=N\ (}$cyclic), ν_{C-N} (cyclic) mode of vibration, respectively.

On the other hand, the position of benzimidazole ν_{N-H} band occurring at ~3150 cm^{-1} gets shifted by 20-25 cm^{-1} to lower frequency region indicating the involvement of -NH group of benzimidazole in coordination to the metal ions. Besides above, the bands due to $\nu_{C=N}$ (azomethine) and ν_{N-N} vibrations also, shift their position in the metal complexes, the former shifting to lower frequency by 10–20 cm^{-1} in all the complexes, implying participation of azomethine nitrogen atom in coordination. Further, an additional band at ~2840 cm^{-1} appears in the IR spectra of the ligand L3 which may be assigned to stretching vibration of –OCH_3 group. The position of this band remains unperturbed in all the complexes indicating non-involvement of –OCH_3 group in co-ordination most probably due to steric reason. Thus, the introduction of –OCH_3 group in ortho position to phenolic –OH does not produce a remarkable change in the IR spectra of the ligand L3 and its complexes. The absorption at ~3500 cm^{-1} may be assigned to ν_{O-H} of co-ordinate or lattice water.

Thermal analysis

The complexes formed by the ligands follow a similar pattern of thermal decomposition. All the complexes lose water in the temperature range below 100 °C indicating them to have lattice water in conformity with analytical and IR spectral data. The loss of water is equivalent to two molecules for Cu(II) complexes while it is equivalent to one molecule for other complexes [26]. The anhydrous complexes follow two stage decompositions between 210 – 315 °C and 340 – 510 °C. The degradation of organic constituents continues until finally the stable metal oxide is obtained. The temperature range of decomposition, peak temperature and the possible fragments removed, have been incorporated in Table 2. The calculation of mass losses from the thermogram leads us to propose the following stoichiometric decomposition scheme for metal complexes of various ligands which are presented below. The mass losses due to the organic constituents have been expressed regarding the mass of the ligands.

1. $ML_2.\ nH_2O$, where, L = L1 ($C_{15}N_4OH_{13}$), M = Co, Ni, Cu and Zn

I. $ML_2.nH_2O\ (s) \rightarrow ML_2(s) + nH_2O(g)$ (40 - 110 °C)
II. $ML_2(s) \rightarrow ML_{1.004}(s) + 0.996L(g)$ (190 – 340 °C)
III. $ML_{1.004}\ (s) \rightarrow MO(s) + 0.943L(g)$ (315 – 485 °C)

2. $ML_2.nH_2O$, where, L = L2 ($C_{20}N_4OH_{15}$), M = Co, Ni, Cu and Zn

I. $ML_2.nH_2O$ (s) → ML_2 (s) + nH_2O(g) (50 - 110 °C)

II. ML_2 (s)→ $ML_{1.193}$ (s)+ 0.807L(g) (230 – 350 °C)

III. $ML_{1.193}$(s) → MO(s) + 1.144L(g) (335 – 500 °C)

3. $ML_2.nH_2O$, where, L = L3 ($C_{15}N_4O_2H_{13}$), M = Co, Ni, Cu and Zn

I. $ML_2.nH_2O$ (s) → ML_2 (s) + nH_2O(g) (40 - 100 °C)

II. ML_2(s) → $ML_{1.061}$(s) + 0.939 L(g) (192 – 335 °C)

III. $ML_{1.061}$ (s) → MO(s) + 1.004L(g) (310 – 480 °C)

In general, the mass loss in the second stage of degradation in the temperature range 190 – 350 °C is correlated to the detachment of two $C_7N_3H_6$ moieties from the complexes by cleavage of -N–N- bond, thereby releasing 2-aminobenzimidazolyl fragments from the anhydrous metal complexes. This may be the consequence of relatively weak nature of –N-N– bond of the ligand due to lone pair-lone pair repulsion between two vicinal nitrogen atoms. This step of degradation requires a little higher temperature in case of complexes with L2 ligands than others, which is believed to be due to the strengthening of –N–N– bond as a result of conjugation with α-phenyl group. The final stage involves the complete elimination of the rest of the organic constituents from the complexes leading to the formation of their respective metal oxides. The temperature range of degradation of the complexes reveals the following order of thermal stability for complexes with different ligands.

L1 complexes: Zn (II) < Co (II) < Ni (II) < Cu (II)
L2 complexes: Co (II) < Ni (II) < Zn (II) < Cu (II)
L3 complexes: Zn (II) < Co (II) < Ni (II) < Cu (II)

Kinetics of the decomposition of complexes

The kinetic parameters such as the order and the activation energies of the decomposition processes of the complexes have been evaluated using Horowitz and Metzger procedure [27]. The following equation has been used for the purpose.

$$\ln\left[\frac{(W_0-W_f)}{(W-W_f)}\right] = \left(\frac{E^{\#}}{RT_s^2}\right)T \quad (1)$$

where, W = the weight remaining at a particular temperature, W_0 = the initial weight and W_f = final weight after the completion of the reaction, $E^{\#}$ = activation energy in kJ mol^{-1}, R = gas constant, and T_s = the DTG peak temperature of decomposition and T = any given temperature.

The plot of $\ln\left[\frac{(W_0-W_f)}{(W-W_f)}\right]$ vs T gives good straight line for each decomposition step, from the slope of which the activation energy $E^{\#}$ has been calculated. The order of the reaction 'n' for each decomposition step has been obtained from the equation $C_s = (n)^{\frac{1}{1-n}}$, where C_s is the weight fraction of the substance present at the DTG peak temperature; T_s, which is given by:

$$C_s = \left[\frac{(W-W_f)}{(W_0-W_f)}\right] \quad (2)$$

The C_s values for all the decomposition steps for each complex are found to be in the range 0.28 – 0.33 which suggests [28] that the thermal reactions follow first order kinetics. The kinetic data of Cu(II) complexes are incorporated in Table 3.

Table 2. Thermo-analytical results of metal complexes.

Metal complex	Molar mass	Temp. range (°C)	Peak temp (°C)	Mass loss found calc. (%)	Removed species	Metallic residue found (Calc.%)
$[Co(L1)_2].H_2O$	606.93	50 – 95	77	2.75 (2.97)	H_2O	CoO 11.98 (12.35)
		210 -318	267	44.12 (43.50)	$2C_7N_3H_6$	
		325-462	410	40.94 (41.19)	$C_{16}N_2OH_{14}$	
		468-509	485			
$[Ni(L1)_2].H_2O$	606.69	55 – 105	80	2.79 (2.97)	H_2O	NiO 11.93 (12.31)
		212 – 330	275	44.23 (43.51)	$2C_7N_3H_6$	
		336 – 470	416	40.66 (41.21)	$C_{16}N_2OH_{14}$	
		485 – 515	497			
$[Cu(L1)_2].2H_2O$	629.5	60 – 110	85	5.38 (5.72)	$2H_2O$	CuO 12.25 (12.63)
		220 -342	295	42.16 (41.94)	$2C_7N_3H_6$	
		345-485	425	38.94 (39.71)	$C_{16}N_2OH_{14}$	
		500-525	514			
$[Zn(L1)_2].H_2O$	613.38	45 – 100	75	2.69 (2.93)	H_2O	ZnO 13.01 (13.27)
		195 -310	259	42.92 (43.04)	$2C_7N_3H_6$	
		318 – 452	403	39.94 (40.76)	$C_{16}N_2OH_{14}$	
		460 – 502	478			
$[Co(L2)_2].H_2O$	730.93	50 – 100	79	2.31(2.46)	H_2O	CoO 10.21 (10.25)
		230 – 325	276	36.65(36.12)	$2C_7N_3H_6$	
		335 -470	415	50.92(51.17)	$C_{26}N_2OH_{18}$	
		480 – 512	493			
$[Ni(L2)_2].H_2O$	730.69	53 – 103	80	2.29 (2.46)	H_2O	NiO 10.15(10.22)
		235 – 332	281	36.89 (36.13)	$2C_7N_3H_6$	
		340 – 477	422	50.52 (51.18)	$C_{26}N_2OH_{18}$	
		482 – 518	497			
$[Cu(L2)_2].2H_2O$	753.5	62 – 112	88	4.35 (4.78)	$2H_2O$	CuO 10.32(10.55)
		242 – 348	301	35.69 (35.04)	$2C_7N_3H_6$	
		355 – 490	431	48.98 (49.64)	$C_{26}N_2OH_{18}$	
		508 – 530	518			
$[Zn(L2)_2].H_2O$	737.38	55 – 110	85	2.31 (2.44)	H_2O	ZnO 10.95 (10.57)
		239 – 339	292	35.58 (35.80)	$2C_7N_3H_6$	
		348 – 485	428	51.94 (51.18)	$C_{26}N_2OH_{18}$	
		497 – 523	505			
$[Co(L3)_2].H_2O$	638.93	42 – 92	76	2.58 (2.82)	H_2O	CoO 11.22 (11.73)
		205 – 312	264	42.18 (41.32)	$2C_7N_3H_6$	
		320 – 455	405	43.98 (44.14)	$C_{16}N_2O_3H_{14}$	
		460- 502	482			
$[Ni(L3)_2].H_2O$	638.69	48 – 95	78	2.55 (2.82)	H_2O	NiO 11.25 (11.69)
		209 – 318	270	42.12 (41.33)	$2C_7N_3H_6$	
		325 – 465	410	43.83 (44.15)	$C_{16}N_2O_3H_{14}$	
		472 – 510	487			
$[Cu(L3)_2].2H_2O$	661.5	55 – 104	82	5.08 (5.44)	$2\ H_2O$	CuO 12.01 (12.02)
		215 – 338	284	40.67 (39.91)	$2C_7N_3H_6$	
		344 – 480	419	41.83 (42.63)	$C_{16}N_2O_3H_{14}$	
		491 – 520	508			
$[Zn(L3)_2].H_2O$	645.38	44 - 95	74	2.46 (2.79)	H_2O	ZnO 12.20 (12.61)
		192 - 307	256	40.68 (40.91)	$2C_7N_3H_6$	
		312 - 445	400	42.98 (43.70)	$C_{16}N_2O_3H_{14}$	
		453 - 498	472			

Table 3. The kinetic data of thermal decomposition of Cu(II) complexes.

Complexes	Decomposition temperature (^oC)	$E^{\#}$ (kJmol^{-1})	C_s
$[Cu(L1)_2].2H_2O$	333-383	83.1	0.31
	493-615	126	0.30
	618-758	247	0.29
	773-798	551	0.31
$[Cu(L2)_2].2H_2O$	335-385	78.4	0.28
	515-621	147	0.30
	628-763	312	0.29
	781-803	504	0.29
$[Cu(L3)_2].2H_2O$	328-377	72.2	0.31
	488-611	134	0.29
	617-753	297	0.28
	764-793	476	0.30

Electronic spectra and magnetic properties

The electronic spectra of Co(II) complexes in DMSO contain two main bands, a broad and a strong band around ~10,500 cm^{-1} (952 nm) and ~22,050 cm^{-1} (453 nm), respectively. The former band can be attributed to $^4T_{1g}(F) \rightarrow {}^4T_{2g}(F)$ (ν_1) and the later to $^4T_{1g}(F) \rightarrow {}^4T_{1g}$ (P) (ν_3) transitions, respectively. The $^4T_{1g}(F) \rightarrow {}^4A_{2g}(F)$ (ν_2), being a two electron transition ($t^5_{2g}\, e^2_g \rightarrow t^3_{2g}\, e^4_g$) involves significant amount of energy, and hence is not observed [29]. The ligand field parameters of the complexes have been calculated by the crystal field approximation [30]. The spectral data of Co(II) complexes reveal that the ligand L3 produces the strongest ligand field around Co(II) ion as evident from the 10 Dq values and the order of ligand field strength is L3 > L1 > L2, which may be attributed to the presence of electron releasing –OCH_3 group in ortho position to –OH of vanillinidene moiety of L3, -CH_3 group (+I effect) in α carbon atom of the salicylidene part of L1 and electron withdrawing –C_6H_5 group (-I effect) in the same position of salicylidene moiety of L2. Further, the inter electron repulsion parameter (B) and nephelauxetic ratio (β) data [30] suggest that the degree of covalency in the complexes follow the order $[Co(L2)_2]\, H_2O$ > $[Co(L1)_2]\, H_2O$ > $[Co(L3)_2]\, H_2O$. The greater delocalization of d- electron charge cloud of Co (II) in $[Co(L2)_2]\, H_2O$ is ascribed to the presence of a phenyl ring in the α position of the salicylidene moiety of the ligand which can accommodate the expanded d-electron charge cloud into its π molecular orbital. The electronic spectral data along with ligand field and nephelauxetic parameters of Co(II) complexes are presented in Table 4.

The electronic spectral data and the magnetic moment values of Ni(II) complexes are presented in Table 5. The spectra of the complexes are found to possess a split band system at ~ 8,600 cm^{-1} (1162 nm) and ~ 10,200 cm^{-1} (980 nm) followed by two main bands at ~ 15,500 cm^{-1} (645 nm) and ~ 24,350 cm^{-1} (410 nm). The last two bands may safely be assigned to $^3A_{2g}(F) \rightarrow {}^3T_{1g}(F)$ (ν_2) and $^3A_{2g}(F) \rightarrow {}^3T_{1g}(P)$ (ν_3) transitions, respectively, under octahedral field. The transition ratio ν_3/ν_2 is however less than expected (~1.7) for octahedral Ni(II) species. This decrease in value may be due to some tetragonal distortion represented by the extent of splitting of ν_1 band. This fact is further supported by the first two bands in the spectrum, which may be split components of ν_1 band under D_{4h} geometry. These split components can be assigned to $^3B_{1g} \rightarrow {}^3E_g$ for band at ~8,600 cm^{-1} and $^3B_{1g} \rightarrow {}^3B_{2g}$ for the band at ~10,200 cm^{-1}, respectively. Tetragonal parameters D_t, D_q^E and D_q^A of Ni (II) complexes are calculated by known method [31] and are incorporated in Table 5. In all the complexes the out-of- plane crystal field strength (D_q^A) is found to be greater than the in-plane one (D_q^E) which

suggests that the axial benzimidazolyl nitrogen binds strongly to the metal centre than the equatorial frame work of two nitrogen and two oxygen in the square plane. Both the axial and equatorial crystal field strength in all the complexes follow the order $[Ni(L3)_2]\ H_2O$ > $[Ni(L1)_2]\ H_2O$ > $[Ni(L2)_2]\ H_2O$. This is consistent with the magnetic moment data which reveal that $[Ni(L2)_2]\ H_2O$ is most paramagnetic owing to the relatively weaker crystal field produced by L2 ligand. The observed μ_{eff} values agree reasonably well with the calculated values [32] using the formula: $\mu_{eff} = \mu_{s.o}(\ 1 - \alpha\lambda/10D_q)$, where $\alpha = 4$ and $\lambda = -315\ cm^{-1}$ for Ni(II) and $10D_q$ is the energy separation between the ground state and the first excited state corresponding to $^3B_{1g}\ (^3A_{2g}) \rightarrow\ ^3E_g\ (^3T_{2g})$ transition. The magnetic moment observed in this case (2.83 – 3.2 BM) corresponds to six coordinate octahedral Ni(II) species.

Table 4. Absorption spectra, ligand field parameters, bending parameter(x) and nephelauxetic parameters of Co(II) complexes.

Complexes	Absorption bands (cm^{-1})			D_q (cm^{-1})	$10D_q$ (cm^{-1})	B (cm^{-1})	β (B/B_0)	X (cm^{-1})
	ν_1 $^4T_{1g} \rightarrow\ ^4T_{2g}$	ν_2 $^4T_{1g} \rightarrow\ ^4A_{2g}$	ν_3 $^4T_{1g} \rightarrow\ ^4T_{1g}(P)$					
$[Co(L1)_2]\ H_2O$	10500	_	22050	1187.3[a] 1179.6[b]	11873[a] 11796[b]	848[a] 853[b]	0.873[a] 0.878[b]	1003
$[Co(L2)_2]\ H_2O$	10230	_	21110	1155.1[a] 1147.5[b]	11551[a] 11475[b]	797[a] 808[b]	0.821[a] 0.832[b]	990
$[Co(L3)_2]\ H_2O$	11060	_	22850	1271.3[a] 1241.0[b]	12713[a] 12410[b]	859[a] 876[b]	0.885[a] 0.902[b]	890

[a]graphical method, [b]Konig's method

Table 5. Electronic spectral data (in cm^{-1}), magnetic moment values and tetragonal parameters of Ni(II) complexes**.**

Complexes	$\nu_1(^3A_{2g} \rightarrow\ ^3T_{2g})$		ν_2 $^3A_{2g} \rightarrow\ ^3T_{1g}$	ν_3 $^3A_{2g} \rightarrow\ ^3T_{1g}$ (P)	D_t (in cm^{-1})	D_q^E (in cm^{-1})	D_q^A (in cm^{-1})	μ_{eff} (in BM)
	$^3B_{1g} \rightarrow\ ^3E_g$	$^3B_{1g} \rightarrow\ ^3B_{2g}$						
$[Ni(L1)_2].H_2O$	8600	10200	15500	24350	-182.9	860	1180	3.25[a] 3.24[b]
$[Ni(L2)_2].\ H_2O$	8250	9875	15150	23860	-185.7	825	1150	3.31[a] 3.26[b]
$[Ni(L3)_2].\ H_2O$	9070	10850	16100	24950	-203.4	907	1263	3.20[a] 3.22[b]

[a]calculated, [b]observed.

The electronic spectra of all the Cu(II) complexes in DMSO are similar in nature. Here the spectra is characterized by two bands at ~14,200 cm^{-1} (704 nm) and ~16,810 cm^{-1} (594 nm) which may be attributed to $^2B_{1g} \rightarrow\ ^2B_{2g}$ (ν_2) and $^2B_{1g} \rightarrow\ ^2E_g$ (ν_3) transitions, suggesting there by a distorted octahedral geometry for these complexes. In this case also the band due to $^2B_{1g} \rightarrow\ ^2A_{1g}$ is not observed most probably due to superimposition by ν_2 band owing to its broadness. The mean value of the two absorptions (ν_2 and ν_3) gives us the tentative 10Dq of the complexes. The absence of any band below ~10,000 cm^{-1} rules out the possibility of tetrahedral or pseudo-tetrahedral geometry. The μ_{eff} values in these cases lie in the range 1.79-1.90 B.M. which is normal for hexa coordinated Cu(II) complexes. The spectral data and magnetic moment values of Cu(II) complexes are reported in Table 6.

Table 6. The electronic spectral bands (in cm^{-1}) and magnetic moment values (μ_{eff}) of Cu(II) complexes.

Complexes	ν_1 $^2B_{1g}\rightarrow{}^2A_{1g}$	ν_2 $^2B_{1g}\rightarrow{}^2B_{2g}$	ν_3 $^2B_{1g}\rightarrow{}^2E_g$	10 Dq (in cm^{-1})	μ_{eff} (in BM)
$[Cu(L1)_2]\,2H_2O$	_	14200	16810	15505	1.83
$[Cu(L2)_2]2H_2O$	_	13950	15870	14910	1.91
$[Cu(L3)_2]\,2H_2O$	_	14550	16900	15725	1.81

NMR spectra

The ^1H NMR spectrum of the ligands displays a multiplet in the region δ 7.6-8.5 ppm corresponding to 8/13/7 aromatic protons of the phenyl groups in L1, L2 and L3, respectively while the signals due to ring NH proton and exocyclic NH proton appear at δ 6.7 ppm and δ 9.0 ppm respectively. Besides the above peaks, a sharp signal at δ 8.7 ppm and δ 4.5 ppm observed due to azomethine (-N=CH-) protons and $-OCH_3$ group respectively in the ligand L3. A signal is also observed in case of ligand L1 due to $–CH_3$ protons, at δ 2.5 ppm. The signal due to ring -NH proton shows a downfield shift appearing at δ 7.0 ppm indicating coordination through the ring -NH group of benzimidazolyl moiety in the complexes. The disappearance of the signal due to the phenolic -OH protons and the downfield signal due to the azomethine protons in the corresponding complexes, indicate the co-ordination of the phenolic oxygen (through deprotonation) and azomethine nitrogen to the metal ion. The IR spectra corroborated the same result. In the ^{13}C NMR spectrum, signals appeared in the region 106.6 to 156.3 are due to aromatic carbons. The signals at 173.1, 161.2 and 19.7 are assigned to C=N (azomethine), C=N (benzimidazole moiety) and CH_3, respectively.

ESR spectra

The ESR spectra of copper complexes were recorded in DMSO at 300 K. The nature of the spectra is similar for all the complexes, which exhibit a well resolved four line spectrum and no features characteristic for a binuclear complex. This is also supported by the magnetic moment of copper complex which confirms the mononuclear nature of the complex. The spin Hamiltonian parameters for the copper complex were calculated from the spectrum. The observed order (g_{11} = 2.23 > $g_\perp$ = 2.08 > 2.0023) indicates that the complex has octahedral geometry [33]. This also suggests that the unpaired electron exists in $d_{x^2-y^2}$ orbital [34], as is evident from the value of the exchange interaction term G, estimated from the expression: G = $\frac{(g_\parallel - 2.0023)}{(g_\perp - 2.0023)}$, i.e., G = 3.28 < 4.0. Here, g_{11} < 2.3 explains the covalent nature of the M→L bonding [35]. The covalency parameter α^2 (= 0.44) is also calculated by using the following expression, which also suggests the covalent nature of the copper complexes.

$$\alpha^2 = \left(g_\parallel - 2.0023\right) + \frac{3}{7}\left(g_\perp - 2.0023\right) + \left(\frac{A_\parallel}{0.036}\right) + 0.04 \quad (3)$$

Antibacterial activity

The ligands show moderate activity against all organisms, whereas the complexes are more active than that of the free ligand. This may be explained on the basis of chelation theory. The structure of the compounds mainly possess C=N bonds, which coordinate to central metal ion. We know, coordination reduces polarity [36] of the metal ion due to the partial sharing of its charge with the donor groups. This process increases the lipophilic nature of the central metal atom. In addition, many other factors like nature of the ligand, solubility, dipole moment, conductivity and geometry may be responsible for the higher antibacterial activity of these metal complexes [37, 38]. The comparative antibacterial activities of the metal complexes with L1, L2 and L3 are shown in Figure 2, 3 and 4.

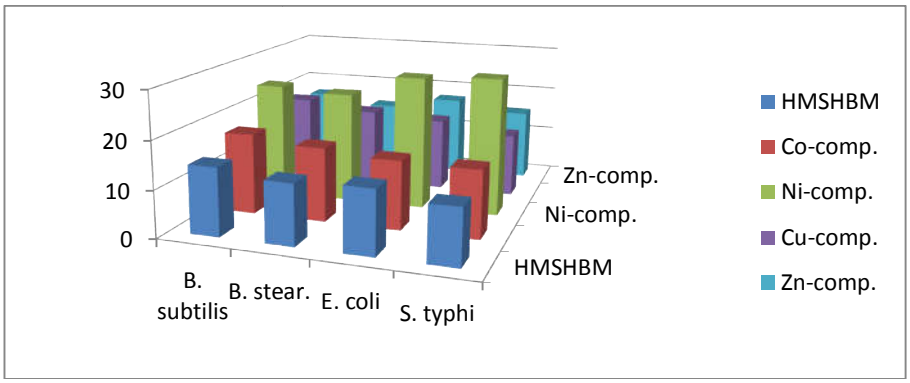

Figure 2. Comparative aspects of antibacterial findings with L1 ligand.

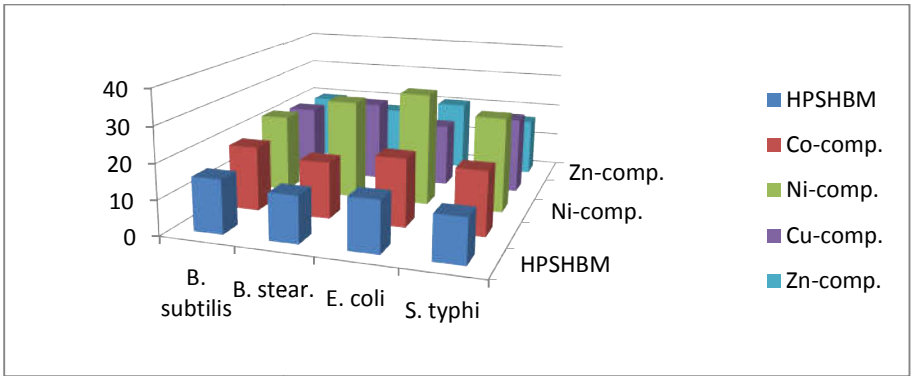

Figure 3. Comparative aspects of antibacterial findings with L2 ligand.

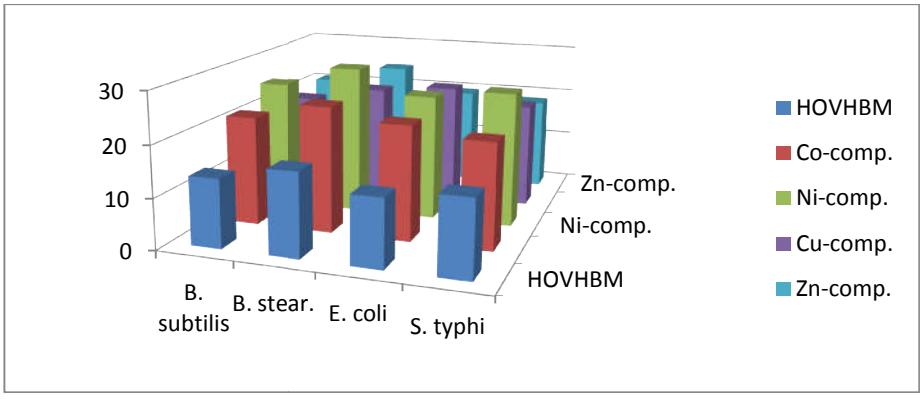

Figure 4. Comparative aspects of antibacterial findings with L3 ligand.

CONCLUSION

The foregoing observations suggest that all the complexes are neutral in nature which is evident from their extremely low values of conductivity. Most of the complexes contain water molecules in their lattice, which certainly do not participate in coordination to the central metal ions as indicated from their thermal behavior. They are removed at a much lower temperature than the coordinated molecules. This is further corroborated from IR spectral investigations. The octahedral geometry of all the complexes are established with tridentate chelation of ligand with azomethine nitrogen, ring nitrogen and oxygen atoms. All these Schiff bases and their metal complexes have been screened for their antibacterial activities. The complexes showed good antibacterial activity compared to the ligands. This may be explained due to enhanced lipophilic property of the central metal ion as a result of chelation with the ligand moieties.

ACKNOWLEDGEMENT

The authors gratefully acknowledge the services rendered by Director, Regional Sophisticated Instrumentation Center, I.I.T., Madras, for recording the spectra.

REFERENCES

1. Ozkay, Y.; Tunai, Y.; Karaka, H.; Isikdag, I. Antimicrobial activity and a SAR study of some novel benzimidazole derivatives bearing hydrazone moiety. *Eur. J. Med. Chem.* **2010**, 45, 3293-3298.
2. Ahmadi, A. Synthesis and antibacterial evaluation of some novel Mannich bases of benzimidazole derivatives. *Bull. Chem. Soc. Ethiop.* **2016**, 30, 421-425.
3. Odame, F.; Krause, J.; Hosten, E.C.; Betz, R.; Lobb, K.; Tshentu, Z.R.; Frost, C.L. Synthesis, characterization and DPPH scavenging activity of some benzimidazole derivatives. *Bull. Chem. Soc. Ethiop.* **2018**, 32, 271-284.
4. Salahuddin; Shaharyar, M.; Mazumder, A.; Ahsan, M. J. Synthesis, characterization and anticancer evaluation of 2-(naphthalen-1-ylmethyl/naphthalen-2-yloxymethyl)-1-[5-(substituted phenyl)-[1,3,4]oxadiazol-2-ylmethyl]-1H-benzimidazole. *Arabian J. Chem*. 2014, 7, 418-424.
5. Sreena, K.; Ratheesh, R.; Rachana, M.; Poornima, M.; Shyni, C. Synthesis and anthelmintic activity of benzimidazole derivatives. *Hygeia* **2009**, 1, 21-22.
6. Noolvi, M.; Agrawal, S.; Patel, H.; Badiger, A.; Gaba, M.; Zambre, A. Synthesis, antimicrobial and cytotoxic activity of novel azetidine-2-one derivatives of 1H-benzimidazole. *Arabian J. Chem.* **2014**, 7, 219-226.
7. Achar, K.C.; Hosamani, K.M.; Seetharamareddy, H.R. In-vivo analgesic and anti-inflammatory activities of newly synthesized benzimidazole derivatives. *Eur. J. Med. Chem.* **2010**, 45, 2048-2054.
8. Cho, S.Y.; Kang, S.K.; Kim, S.S.; Cheon, H.G.; Choi, J.K.; Yum, E.K. Synthesis and SAR of benzimidazole derivatives containing oxycyclic pyridine as a gastric H^+/K^+ -ATPase inhibitors. *Bull. Korean Chem. Soc.* **2001**, 22, 1217-1223.
9. Tonelli, M.; Paglietti, G.; Boido, V.; Sparatore, F.; Marongiu, F.; Marongiu, E.; La Colla, P.; Loddo, R. Antiviral activity of benzimidazole derivatives. I. Antiviral activity of 1-substituted-2-[(benzotriazol-1/2-yl)methyl]benzimidazoles. *Chem. Biodivers.* **2008**, 5, 2386-2401.
10. Shingalapur, R.V.; Hosamani, K.M.; Keri, R.S.; Hugar, M.H. Derivatives of benzimidazole pharmacophore: Synthesis, anticonvulsant, antidiabetic and DNA cleavage studies. *Eur. J. Med. Chem.* **2010**, 45, 1753-1759.

11. Mohapatra, R.K.; Dash, M.; Mishra, U.K.; Mahapatra, A.; Dash, D.C. Synthesis and characterization of transition metal complexes with benzimidazolyl-2-hydrazones of glyoxal, diacetyl and benzil. *Synth. React. Inorg. Metal-Org. Nano-Met. Chem*. **2014**, 44, 642-648.
12. Mohapatra, R.K.; Mishra, U.K.; Mishra, S.K.; Mahapatra, A.; Dash, D.C. Synthesis and characterization of transition metal complexes with benzimidazolyl-2-hydrazones of *o*-anisaldehyde and furfural. *J. Korean Chem. Soc*. **2011**, 55, 926-931.
13. Wu, H.; Zhang, J.; Zhang, Y.; Chen, C.; Li, Z.; Wu, M.; Yang, Z. Syntheses, crystal structures, electrochemical studies, and antioxidant activities of zinc(II) and copper(II) complexes with bis(2-benzimidazolyl) aniline derivatives. *J. Coord. Chem*. **2015**, 68, 835-847.
14. Kantchew, E.A.B.; O'Brien, C.J.; Organ, M.G. Palladium complexes of N-heterocyclic carbenes as catalysts for cross-coupling reactions—A synthetic chemist's perspective. *Angew. Chem.* **2007**, 46, 2768-2813.
15. Poyraz, M.; Sari, M.; Guney, A.; Demirci, F.; Demirayak, S.; Sahin, E. Synthesis, characterization and antimicrobial activity of a Zn(II) complex with 1-(1H-benzoimidazol-2-yl)-ethanone thiosemicarbazone. *J. Coord. Chem*. **2008**, 61, 3276-3283.
16. Galal, S.A.; Hegab, K.H.; Kassab, A.S.; Rodriguez, M.L.; Kerwin, S.M.A.; El-Khamry, A-M.; El-Diwani; H.I. New transition metal ion complexes with benzimidazole-5-carboxylic acid hydrazides with antitumor activity. *Eur. J. Med. Chem*. **2009**, 44, 1500-1508.
17. Wu, H.; Yuan, J.; Bal, Y.; Pan, G.; Wang, H.; Shao, J.; Gao, J.; Wang, Y. Synthesis, crystal structure, DNA-binding properties, and antioxidant activity of a V-shaped ligand bis(*N*-methylbenzimidazol-2-ylmethyl)benzylamine and its zinc(II) complex. *J. Coord. Chem*. **2012**, 65, 4327-4341.
18. Zhao, J.; Li, S.; Zhao, D.; Chen, S.; Hu, J. Metal and structure tuned *in vitro* antitumor activity of benzimidazole-based copper and zinc complexes. *J. Coord. Chem*. **2013**, 66, 1650-1660.
19. Streciwilk, W.; Cassidy, J.; Hackenberg, F.; Muller-Bunz, H.; Paradisi, F.; Tacke, M. Synthesis, cytotoxic and antibacterial studies of *p*-benzyl-substituted NHC–silver(I) acetate compounds derived from 4,5-di-*p*-diisopropylphenyl- or 4,5-di-*p*-chlorophenyl-1*H*-imidazole. *J. Organomet. Chem.* **2014**, 749, 88-99.
20. Dash, D.C.; Mahapatra, A.; Mohapatra, R.K.; Ghosh; S.; Naik, P. Synthesis and Characterization of dioxouranium(VI), thorium(IV), oxozirconium(IV) and oxovanadium(IV) complexes with 1,11-dihydroxy-1,4,5,7,8,11-hexaaza-2,3,9,10-tetramethyl-1,3,8,10-decatetraene-6-thione and their derivatives with chloroacetic acid. *Indian J. Chem*. **2008**, 47A, 1009-1013.
21. Mohapatra, R.K. Synthesis and characterization of UO_2(VI), Th(IV) and VO(IV) complexes with a Schiff base and their derivatives with chloroacetic acid. *J. Indian Chem. Soc.* **2010**, 87, 1251-1255.
22. Azam, A.; Al-Resayes, S.I.; Wabaidur, S.M.; Trzesowska-Kruszynska, A.; Kruszynski, R.; Mohapatra, R.K.; Siddiqui, M.R.H. Cd(II) complex constructed from dipyridyl imine ligand: Design, synthesis and exploration of its photocatalytic degradation properties. *Inorg. Chim. Acta* **2018**, 471, 698–704.
23. Mohapatra, R.K.; Ghosh, S.; Naik, P.; Mishra, S.K.; Mahapatra, A.; Dash, D.C. Synthesis and characterization of homo binuclear macrocyclic complexes of UO_2(VI), Th(IV), ZrO(IV) and VO(IV) with Schiff-bases derived from ethylene diamine/orthophenylene diamine, benzilmonohydrazone and acetyl acetone. *J. Korean Chem. Soc*. **2012**, 56, 62-67.
24. Vogel, A.I. *A Hand Book of Quantitative Inorganic Analysis*, 2nd ed., Longman: London; **1969**.

25. El-Ella, D.A.; Gonitzer, E.; Wendelin, W. Synthesis and structural elucidation of pyrimido-[1,2-*a*]benzimidazoles and fused derivatives. I. Dihydropyrimido[1,2-*a*]benz. imidazoles. *J. Heterocycl. Chem.* **1996**, 33, 373-382.
26. Nikolaev, A.V.; Lagvienko, V.A.; Myachina, I. *Thermal Analysis*, Academic Press: New York; **1969**.
27. Horowitz, H.H.; Metzger, G. A new analysis of thermogravimetric traces. *Anal. Chem.* **1963**, 35, 1464-1468.
28. Soliman, A.A.; Linert, W. Investigations on new transition metal chelates of the 3-methoxy-salicylidene-2-aminothiophenol Schiff base. *Thermochim. Acta* **1999**, 338, 67-75.
29. Lever, A.B.P. *Inorganic Electronic Spectroscopy*, Elsevier: New York; **1968**.
30. Reddy, K.V. *Symmetry and Spectroscopy of Molecules*, New Age International Publishers: New Delhi; **2009**.
31. Ray, R.K. *Electronic Spectra of Transition Metal Complexes*, New Central Book Agency: London; **2011**; p 365.
32. Dutta R.L.; Syamal, A. *Elements of Magnetochemistry*, 2nd ed., Affiliated East-West Press Pvt. Ltd.: New Delhi; **1993**; p 69.
33. Nagakavitha, D.; Reddy, K.H. Synthesis, spectral characterization and DNA binding properties of dinuclear copper(II) complexes with pyridinehydrazones. *J. Indian Chem. Soc*. **2015**, 92, 71-78.
34. Raman, N.; Kulandaisamy, A.; Jayesubramanian, K. Synthesis, spectral, redox and biological studies of some Schiff base copper(II), nickel(II), cobalt(II), manganese(II), zinc(II) and oxovanadium(II) complexes derived from 1-phenyl-2,3-dimethyl-4(4-iminopentan-2-one) pyrazol-5-one and 2-aminophenol/2-amino-thiophenol. *Indian J. Chem*. **2002**, 41A, 942-949.
35. Prabhakara, C.T.; Patil, S.A.; Kulkarni, A.D.; Naik, V.H.; Manjunatha, M.; Kinnal, S. M.; Badami, P.S. Synthesis, spectral, thermal, fluorescence, antimicrobial, anthelmintic and DNA cleavage studies of mononuclear metal chelates of bi-dentate 2H-chromene-2-one Schiff base, *J. Photochem. Photobiol. B: Biology* **2015**, 148, 322-332.
36. Balhausen, C.J. *An Introduction to Ligand Field*, McGraw Hill: New York; **1962**.
37. El-Gamel, N.E.A. Metal chelates of ampicillin versus amoxicillin: synthesis, structural investigation, and biological studies. *J. Coord. Chem.* **2010**, 63, 534-543.
38. Shakdofa, M.M.E.; Al-Hakimi, A.N.; Elsaied, F.A.; Alasbahi, S.O.M.; Alkwlini, A.M.A. synthesis, characterization and bioactivity Zn^{2+}, Cu^{2+}, Ni^{2+}, Co^{2+}, Mn^{2+}, Fe^{3+}, Ru^{3+}, VO^{2+} and UO_2^{2+} complexes of 2-hydroxy-5-((4-nitrophenyl) diazenyl)benzylidene)-2-(*p*-tolylamino)-acetohydrazide. *Bull. Chem. Soc. Ethiop.* **2017**, 31, 75-91.